Solute transport in heterogeneous karst systems

Dewaide, Lorraine; Bonniver, Isabelle; Rochez, Gaëtan; Hallet, Vincent

Published in:
Journal of Hydrology

DOI:
10.1016/j.jhydrol.2016.01.049

Publication date:
2016

Document Version
Publisher's PDF, also known as Version of record

Journal of Hydrology 534 (2016) 567–578

Contents lists available at ScienceDirect

Journal of Hydrology

journal homepage: www.elsevier.com/locate/jhydrol

Solute transport in heterogeneous karst systems: Dimensioning and estimation of the transport parameters via multi-sampling tracer-tests modelling using the OTIS (One-dimensional Transport with Inflow and Storage) program

Lorraine Dewaide *, Isabelle Bonniver [1], Gaëtan Rochez, Vincent Hallet

University of Namur, Geology Department, Rue de Bruxelles, 61, 5000 Namur, Belgium

ARTICLE INFO

Article history:
Received 3 July 2015
Received in revised form 21 December 2015
Accepted 19 January 2016
Available online 29 January 2016
This manuscript was handled by Laurent Charlet, Editor-in-Chief, with the assistance of Chong-Yu Xu, Associate Editor

Keywords:
Solute transport
Karst conduit dimensioning
Tracer-test
Transport parameters
Transient storage
Tailing effect

SUMMARY

This paper presents the modelling results of several tracer-tests performed in the cave system of Han-sur-Lesse (South Belgium). In Han-sur-Lesse, solute flows along accessible underground river stretches and through flooded areas that are rather unknown in terms of geometry. This paper focus on the impact of those flooded areas on solute transport and their dimensioning. The program used (One-dimensional Transport with Inflow and Storage: OTIS) is based on the two-region non equilibrium model that supposes the existence of an immobile water zone along the main flow zone in which solute can be caught. The simulations aim to replicate experimental breakthrough curves (BTCs) by adapting the main transport and geometric parameters that govern solute transport in karst conduits. Furthermore, OTIS allows a discretization of the investigated system, which is particularly interesting in systems presenting heterogeneous geometries. Simulation results show that transient storage is a major process in flooded areas and that the crossing of these has a major effect on the BTCs shape. This influence is however rather complex and very dependent of the flooded areas geometry and transport parameters. Sensibility tests performed in this paper aim to validate the model and show the impact of the parametrization on the BTCs shape. Those tests demonstrate that transient storage is not necessarily transformed in retardation. Indeed, significant tailing effect is only observed in specific conditions (depending on the system geometry and/or the flow) that allow residence time in the storage area to be longer than restitution time. This study ends with a comparison of solute transport in river stretches and in flooded areas.

1. Introduction

Tracer tests can be a powerful tool when they are used in a quantitative approach in order to characterize solute transport in karst conduits. They provide direct information about groundwater trajectories and hydraulic connections inside a complex karstic network and give breakthrough curves (BTCs) from which some major transport parameters can be easily assessed (first arrival, travel time, tracer velocity, tracer recovery,...).

Modelling of solute transport in karst conduits consists in fitting a modelled BTC with the one obtained in field experiment. Modelling of BTCs allows to define transport parameters, notably the advection and dispersion effects, to evaluate the active conduit geometry and to predict the behavior of a karstic system in different flow conditions.

The karstic site of Han-sur-Lesse is a major system in Belgium that offers interesting features in a modelling purpose. Indeed, the system corresponds to an entire stream sinking into a hole that can swallow up to 25 m^3/s and flooding a large heterogeneous karstic network made of flooded areas that are interconnected by conduit stretches. Flooded areas are saturated zones of unknown geometry, probably intensely karstified but with limited physical access. The assumption is that the transport dynamic is different in those flooded areas and in the river stretches. Therefore the objectives of this study are firstly to observe and to characterize the solute transport in both the flooded zones and the river stretches; secondly to dimension the active system.

In this aim, the OTIS program (One-dimensional Transport with Inflow and Storage), developed by Runkel (1998), was chosen partly because it offers the possibility to build a discrete system and therefore to test the effect of geometry on solute transport.

* Corresponding author. Tel.: +32 81724475.
E-mail addresses: lorraine.dewaide@unamur.be (L. Dewaide), Vincent.hallet@unamur.be (V. Hallet).
[1] Present address: SPW, DGO 3, Avenue Prince de Liège, 15, 5100 Namur, Belgium.

http://dx.doi.org/10.1016/j.jhydrol.2016.01.049
0022-1694/

Furthermore the Han-sur-Lesse BTCs show an asymmetry, a tailing that is commonly observed in field BTCs in general. This persistent skewness is often associated to retardation in the literature. The process recognized as the main cause of retardation is the existence of immobile flow regions along the tracer path (Hubbard et al., 1982; Martin and McCutcheon, 1998). As OTIS allows the simulation of discrete immobile water zones, this study will also test the effect of transient storage on the BTCs. Finally, sensibility tests will show the efficiency of OTIS as a modelling program for solute transport parametrization and karst conduits dimensioning.

2. The OTIS program: theoretical background

Ground-water flow and solute transport in karst conduits are characterized by turbulent flow in a non-constant permeability media. Classical advection–dispersion Eq. (1) can explain solute transport in karst conduits only in the case of equilibrium model, i.e. in dynamic processes. In equilibrium model, evolution of the solute concentration (C) with time (t) is only dependent on the longitudinal flow velocity (v_L) and their longitudinal dispersion (D_L). Eq. (1) supposes a decay coefficient (μ) that can affect the restitution rate and a retardation factor (R_f) that is here only linked to solute sorption on solid particles.

$$R_f \frac{\partial C}{\partial t} = D_L \frac{\partial^2 C}{\partial x^2} - v_L \frac{\partial C}{\partial x} - \mu C \tag{1}$$

Eq. (1) is however not sufficient to explain transport in karstic systems. Indeed, it can't explain the asymmetry generally observed in field BTCs. This persistent skewness and tailing has been widely discussed and considered as the results of complementary processes as adsorption–diffusion, molecular diffusion, dilution effects, multiple conduits effects, but the main process responsible for BTCs skewness is the interaction with immobile water (Hubbard et al., 1982; De Marsily, 1986; Maloszewski and Zuber, 1989; Rossier and Kiraly, 1992; Maloszewski et al., 1992; Werner et al., 1997). Therefore, transient storage has to be taken into account in Eq. (1). It exists in regular or irregular conduits due to the velocity gradient between the main flow zone and the conduits walls that causes turbulent flow (Martin and McCutcheon, 1998; Hauns and Jeannin, 1998; Hauns et al., 2001). Field and Pinsky (2000) proposed the "two-region non-equilibrium model" that supposes the existence of immobile water zones along the solute transport path. An exchange exists between mobile and immobile zones but transport is only effective in the mobile, dynamic zone. Runkel (1998) developed a program called OTIS (One-dimensional Transport with Inflow and Storage) based on the two-region non-equilibrium approach. OTIS was initially created to solve solute transport problematic in surface streams implying concentration variation in longitudinal direction only and free elevation of the water level, features that are relevant for karst conduit flows. As shown in Fig. 1, OTIS supposes a main dynamic flow in mobile zone in which solute is transported by advection and affected by dispersion and, possibly, adsorption and decay. Next to the main channel, immobile zones equally distributed along the main flow zone exist. They act as transient storage zones for the solute that can be affected by chemical reactions but where there is no transport by advection and dispersion. To permit storage in stagnant zones, an exchange between mobile and immobile water zones has to take place. Finally, lateral flow can be added and/or retract from the main flow.

In accord with all these features, the OTIS program is guided by the following equations for conservative and non-conservative solutes (terms in square brackets):

$$\frac{\partial C}{\partial t} = -\frac{Q}{A}\frac{\partial C}{\partial x} + \frac{1}{A}\frac{\partial}{\partial x}\left(AD_L\frac{\partial C}{\partial x}\right) + \frac{q_{lin}}{A}(C_{lin} - C) + \alpha(C_s - C) + [\rho\lambda'(C_{sed} - K_d C) - \lambda C] \tag{2}$$

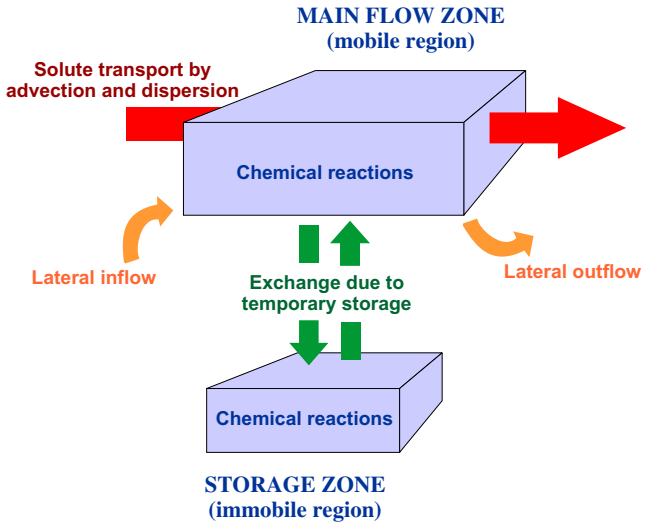

Fig. 1. Main functioning principles in OTIS. Solute transport occurs in the main flow zone while an exchange with a storage zone exists (modified from Runkel, 1998).

and,

$$\frac{\partial C_s}{\partial t} = \alpha\frac{A}{A_s}(C - C_s) + [\lambda'_s(C'_s - C_s) - \lambda_s C_s] \tag{3}$$

where C, C_{lin} and C_s [M/L^3][2] are solute concentrations in, respectively, the main channel, the lateral inflow and the storage zone; A and A_s [L^2] the cross-sectional areas in the main channel and storage zone; Q [L^3/T] the volumetric flow rate; q_{lin} [L^3/T L] the lateral inflow rate; D_L [L^2/T] the longitudinal dispersion coefficient; α [T^{-1}] the storage zone exchange coefficient; t the time [T]; x the distance [L]. Considering non-conservative solute, C_{sed} is the sorbate concentration on sediment; C'_s the background storage zone solute concentration; K_d [L^3/M] the distribution coefficient; λ and λ_s [T^{-1}] the first-order decay in the main channel and the storage zone; λ' and λ'_s [T^{-1}] the sorption rate coefficient in the main channel and the storage zone; ρ [M/L^3] the mass of accessible sediment by volume water.

The major advantage in OTIS is the possibility of discretization of the system which is a very interesting feature in heterogeneous environments. A system needs therefore to be conceptualized in order to be cut in "reaches" that can be modelled separately, and so being characterized by different dimensions and transport parameters. Each reach is subdivided in a number of discrete segments that represent control volumes within which mass is conserved. Eqs. (2) and (3) apply then in each segment and numerical solutions have to be found.

To implement a numerical solution scheme, OTIS uses the implicit Crank-Nicolson method (for details on the solutions, see Runkel, 1998; Runkel and Broshears, 1991). The solution has to be constrained by conditions at the upstream and downstream boundary of the system. The upstream boundary condition (USBC) is the solute concentration injected in the system. This concentration can vary in time regarding to the injection mode (concentration-step, flux-step, concentration-continuous). The downstream boundary condition (DSBC) is not a concentration but a dispersive flux. This flux is defined at the interface between the last segment in the modelled system and an additional fictitious segment. Eventually, to solve the equations that governed the model, it should be precise if the solute is conservative or not (Eqs. (2) and (3) without or with square brackets) and if the transport occurred in steady or unsteady flow.

[2] The fundamental units of Mass [M], Length [L] and Time [T] are used throughout this chapter.

3. Methodology

Quantitative tracer-tests are powerful tools to assess the main features of an active karst system. Indeed, the resulting BTCs parameters inform on the solute transport dynamics within the system. The system investigated in the context of this paper shows very distinct geometric features along the tracer path in the form of river stretches and flooded areas. Therefore, as the OTIS program gives the possibility to subdivide the system in reaches, each heterogeneity in the system can be associated to one different reach characterized by specific dimensions and transport parameters. In order to simulate solute transport in each reach, sampling points must be settled at the upstream and downstream boundaries of those reaches. In practice, each reach is first calibrated independently on basis of the intermediate sampling points; which means that each intermediate BTC is used as USBC. Secondly, the calibrated reaches are assembled in a unique discrete but continuous system in which are considered only one solute introduction at the entrance and an exclusive BTC at the exit (Fig. 2). It is important to precise that the simulations presented below make the assumption that decay and sorption are non-existent along the path (conservative tracer). Consequently, retardation observed in BTCs will not be considered as the result of sorption–desorption effects and, taking into account Eq. (2), the only parameters that intervene in the simulations are the main flow section (A), the storage zone section (A_s), the mass exchange coefficient (α) and the longitudinal dispersion coefficient (D_L).

Calibration of the dimension and transport parameters is the result of trial and error tests (direct method). Once the fitting between the simulated curve and the field data is graphically accurate, a final step of optimization is realized thanks to OTIS-P which is a complementary version of OTIS. The OTIS-P model couples the mathematical framework of OTIS with the Nonlinear Least Square algorithms of STARPAC (for details see Runkel, 1998; Donaldson and Tryon, 1990). This leads to an automated parameter estimation (inverse method). However, one should understand that this inverse determination of parameters comes after the trial–error tests. Indeed, to run OTIS-P, a first parameter estimation is needed. Therefore, this optimization process is rather constrained by the direct estimation which takes into account the observations made on the field.

Sensibility tests are systematically realized to evaluate the reliability of the modelled parameters values. They consist in varying one parameter at a time, the others staying constant. Furthermore, the numerical stability of the model can be verified by two parameters: the numerical Current (C_r) and Peclet (P_e). They are defined as follow (Gray and Pinder, 1976; Kinzelbach, 1986):

$$C_r = \frac{v \cdot \Delta t}{\Delta l}, \text{ and, } P_e = \frac{v \cdot \Delta l}{D_L}$$

where v is the particle effective velocity, Δt the integration timestep, Δl the length of the discrete element and D_L the longitudinal dispersion. C_r should be inferior to 1 to ensure that the advection transport length is smaller than the discrete element length, so that the concentration variation due to advection is visible within this element. P_e expresses the equilibrium between advection and dispersion within the discrete element. It shouldn't exceed the value of 2 for a stable model.

A complete OTIS model can then finally be proposed and the results analyzed and criticized. At last, the accuracy of the model can be validated in applying this model to other tracer-tests realized in different flow conditions.

As stated in the introduction, the following chapters will show applications of the OTIS model in the case of the Han-sur-Lesse cave system. Next chapters will give a brief geological and karstic setting, the main results of the tracer-tests and the OTIS simulation assumption and optimized results.

4. Geologic and hydrogeologic settings

Han-sur-Lesse is a small village located in South Belgium, about 60 km south-west from the city of Namur. The Han-sur-Lesse karstic network is developed in the belgian Givetian limestones outcropping within a geomorphological unit called "La Calestienne" that forms a high relief in the landscape in contrast to the surrounding siltstones. More specifically, the cave appears in the "Boine Massif", a 1.6 km^2 ridge of fractured limestones. This ridge corresponds to an anticlinal dome oriented E–W and with a westward plunge. Major faults and fractures follow either a NE–SW or a NNW–SSE direction. The complex structure of the Boine Massif is inherited from the variscan and meso-cenozoïcan tectonics and the cave network is follows mainly the intensely fractured fold axis (Fig. 3). Given a strong relationship with the structural and lithological features, the sub-vertical stratification plans favor here a vertical development of the karst features (Havron et al., 2007).

The drainage of the massif is mainly supported by the 2 km long sinkhole-resurgence system between the Gouffre de Belvaux (GB) and the Trou de Han (TH). The active karst system is sustained by the surface Lesse river that drains a flow varying between 0.5 and 90 m^3/s. When the discharge of the river is less than 25 m^3/s, it sinks entirely into the swallow hole which is perched above the groundwater level. When the surface flow exceeds 25 m^3/s however, the sinkhole is saturated and overflows into the aerial waterway (Quinif, 1988) where downstream sinkholes can be activated. The system consists in subterraneous river stretches that connect flooded areas (Fig. 4). While the river stretches are rather well known because of their speleological access, the flooded areas can only be explored by diving. Those areas can be described as permanently saturated zones, hundreds of meters long and that can reach at least 40 m below the resurgence level in deepness. They consist in interconnected heterogeneous flow sections that develop in highly fractured and karstified rock volumes (Bonniver, 2011). Due to the high degree of karstification, the regional piezometric gradient of the limestone aquifer is less than 0.1%. The exact geometry of these flooded areas is unknown.

5. Solute transport features

5.1. Multi-sampling site tracer-test: first model building

As explained above, the karstic network in Han-sur-Lesse is very well known and precise topographic data are available. However, the flooded areas remain a question mark regarding their dimensions and their influence on solute transport. They can be described as irregular saturated zones embedded in fracturated stones and rocks of various volumes. Due to intense karstification, the top of these areas is at the atmospheric pressure. Given this erratic geometry, they should involve immobile water zones in which the solute is temporarily caught and can be exchange with the main flow zone. In contrast, river stretches are usual karst conduit where an actual river flows and where, according to field observation, transient storage in immobile water zones is either a minor or non-existent process. Therefore, in order to find how the transport parameters behave in flooded areas and in river stretches, modelling of those sections and their associate parameters is needed.

To address to this issue, a tracer-test was performed in low flow conditions in order to characterize solute transport between the Gouffre de Belvaux (GB) and the Trou de Han (TH). However, for practical reasons not developed here, the system considered for

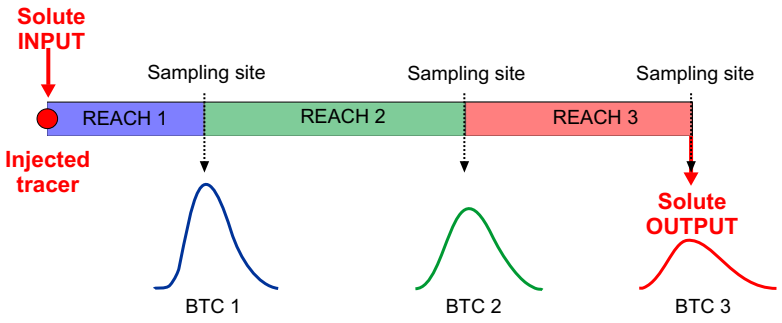

①

Calibration	USBC	DSBC
Reach 1	injected tracer	BTC 1
Reach 2	BTC 1	BTC 2
Reach 3	BTC 2	BTC 3

②

Discretization	USBC	DSBC
Whole system (reaches 1, 2,3)	Solute INPUT (Injected tracer)	Solute OUTPUT (BTC3)

Fig. 2. Modelling principle. First, calibration is realized on each reach individually; then the final discretization simulate solute transport on the whole system. Optimization is a complementary process not shown in this figure.

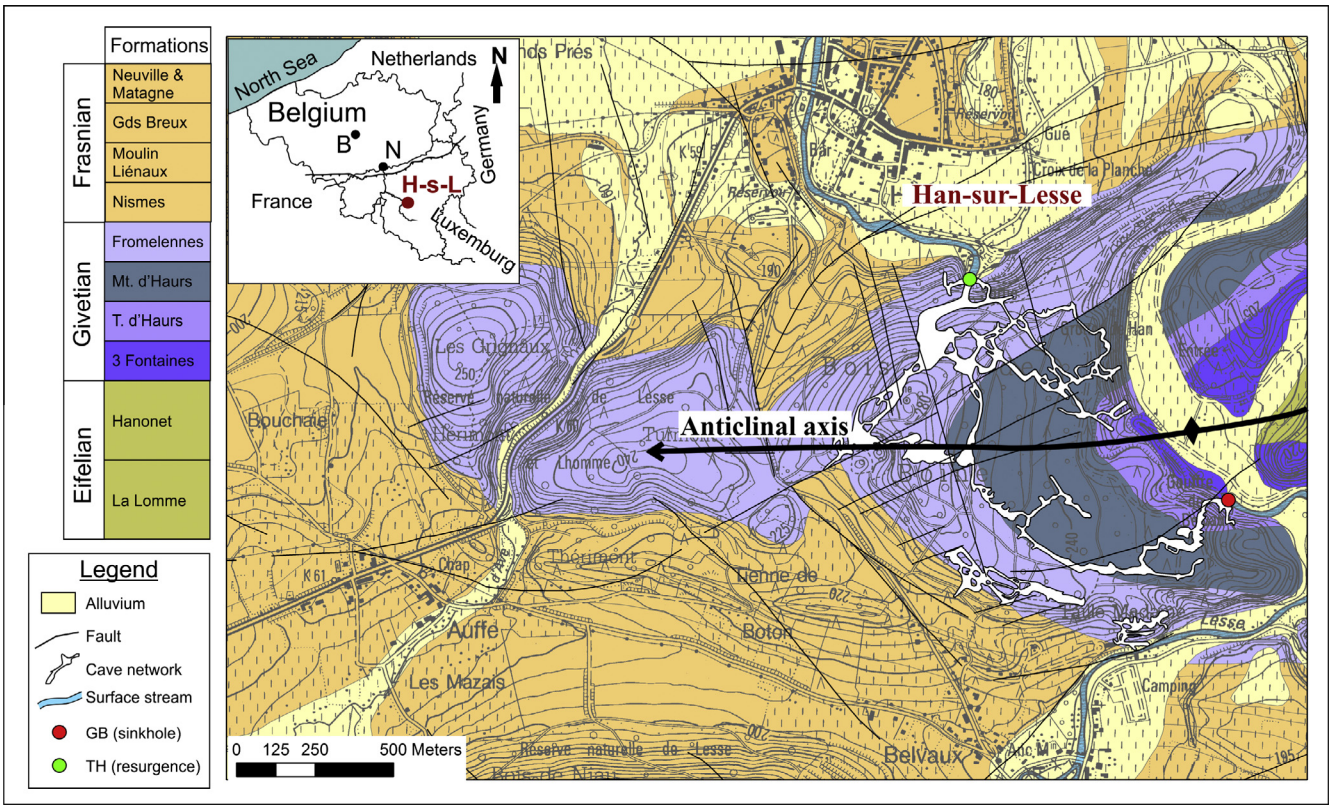

Fig. 3. Location and geological setting of the Han-sur-Lesse karstic network. Karst is developed mainly along the intensely fractured fold axis in the Givetian limestones. [B]: Brussels, [N]: Namur, [H-s-L]: Han-sur-Lesse (modified from Blockmans and Dumoulin, in press).

dimensioning is limited between GB and location C. The total length of this system (GB–C) is about 1.5 km. The measured discharge was of 0.7 m^3/s. The flow was stable along the tracer path (no lateral inflow) and the discharges stayed steady during all the restitution period. 200 g of fluorescein was injected 260 m upstream the GB to assure a good homogenization of the tracer cloud before its entry in the system. Four automatic sampling and measuring devices (fluorometers GGUN-FL30, Schnegg and Doerfliger, 1997) were placed along the system and define three sub-systems of different length. Sub-systems GB–A and B–C correspond to flooded areas that are connected by the river stretch subsystem A–B (Fig. 5).

Restitution rate at the output was of 85%, meaning that the losses are very poor. Given the modelling objective based on this tracer-test, BTCs obtained at each sampling site were corrected for a tracer recovery set at 100% (Fig. 6). Therefore, it is supposed that there is no loss of the tracer along the system; that the chemical reactions of sorption and decay are non-existent; and that

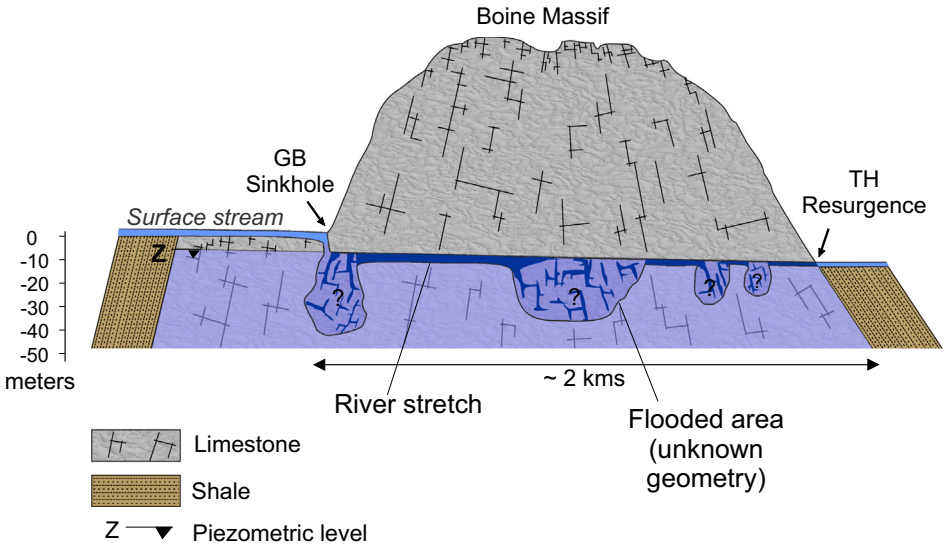

Fig. 4. Cross section in the Boine Massif. The Han-sur-Lesse karstic system is a succession of flooded areas linked by underground river stretches. [GB]: *Gouffre de Belvaux*, [TH]: *Trou de Han*. Dimensions of the flooded zones are hypothetic (modified from Bonniver, 2011).

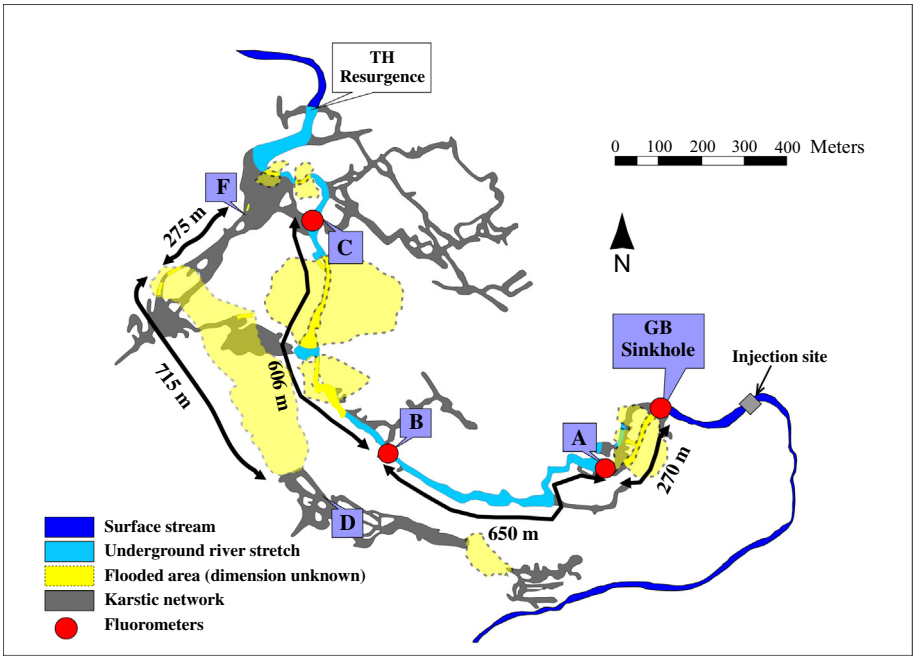

Fig. 5. Tracer-test system divided in subsystems. Sections GB–A and B–C are mainly flooded areas while A–B corresponds to a river stretch. Locations D and F are involved in another test (Section 5.3.2) (modified from Bonniver, 2011).

location C is the only output of the system (which is confirmed by the observations of the geological environment). A qualitative analysis of the BTCs indicates that transport seems dominated by advection (closed and rather symmetric curves) and that the maximum concentration is decreasing along the path while the curves are widening. The growing asymmetry and flattering of the curves are related to retardation and dispersion effects. However, looking at the experimental BTCs shape, there is no clear difference in the behavior of the solute when it crosses the river stretch or the flooded area. The influence of the flooded area will therefore be evaluated through the modelling of the transport parameters. OTIS, allowing a discretization of the system, is a valuable and adequate tool in this purpose.

The conceptual model used to perform transport simulations in the Han-sur-Lesse cave is presented in Fig. 7. Each subsystem of the conceptual model corresponds to one "Reach" in OTIS. Each Reach is divided in segments of 0.5 m length (L_{seg}) in which are performed Eqs. (2) and (3) at an integration time of $8 \cdot 10^{-4}$ h (ΔT). No lateral inflow (q_{lin}) or outflow (q_{lout}) is taken into account as none is known and furthermore there is no discharge variation between the upstream and the downstream flows of the system (steady flow). As the restitution rate considered in the BTCs is 100% (see above), chemical reactions are supposed non-existent (conservative tracer). Storage zone and exchange coefficient are simulated only in reaches corresponding to flooded areas.

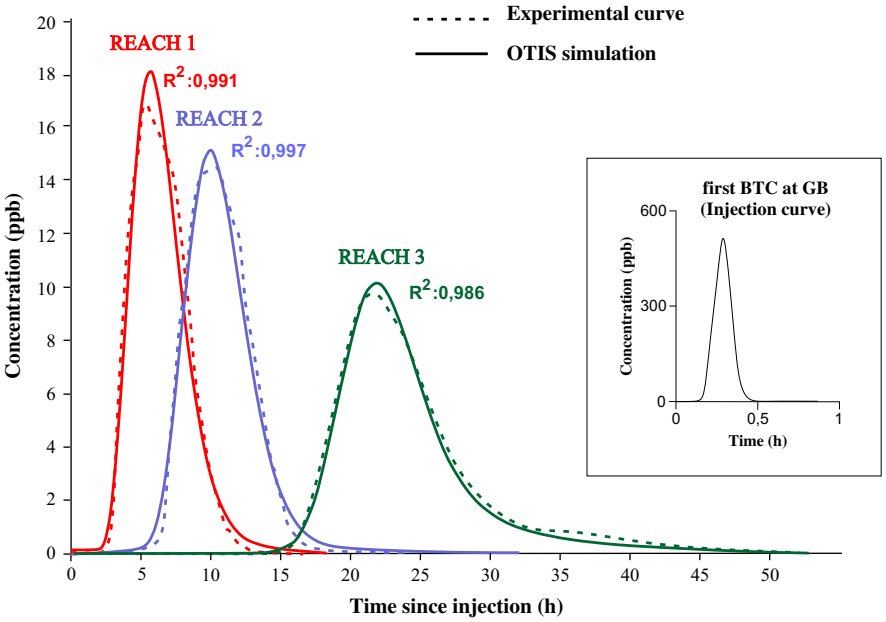

Fig. 6. Tracer-test 1 results. Comparison between experimental BTCs and the curves obtained by calibration of each reach.

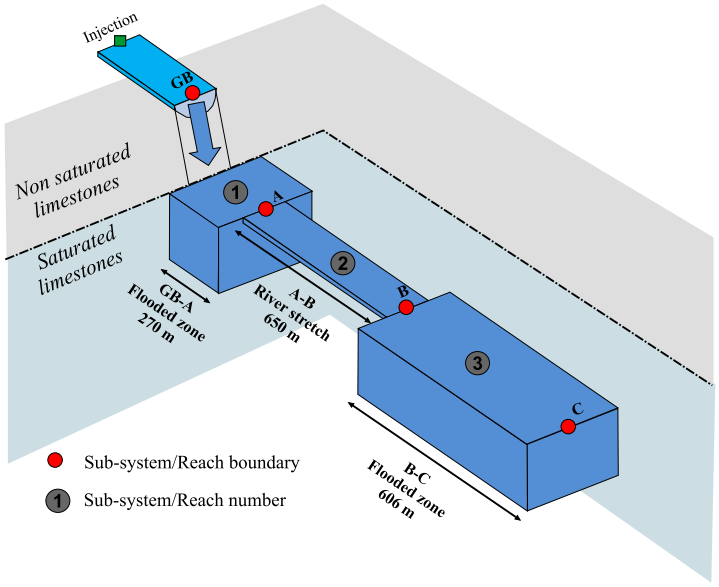

Fig. 7. Conceptual model of the investigated system. Three sub-systems, defined as flooded zone or river stretch, are considered as reaches for the OTIS simulation. Note that the GB sinkhole site is considered as perched in contrast to the subterraneous system (modified from Bonniver, 2011).

Precise calibration of each reach was realized using the upstream BTC as the input and the downstream BTC as the output. Each experimental BTC was therefore simulated via OTIS in fitting the simulated curve to the experimental one, and this fitting was optimized with OTIS-P (Fig. 6) The coefficients of determination have a value of 0.991; 0.997 and 0.986 for reach 1, 2 and 3 respectively. In addition to the conduits dimensioning, the transport parameters are also estimated (Table 1 – tracer-test 1: $Q = 0.7\ m^3/s$). Results are discussed in detail in the following chapter but it can already be said that dimensioning values from Table 1 seem realistic. Indeed, the model estimates the river stretch main flow section at 17 m^2 which is consistent with field observations. A validation of the built model is proposed in the next chapter.

5.2. Model validation and discussion on the parameters

To validate the model, two complementary tracer tests were performed in various hydrological conditions: the second one was conducted for a river discharge of 0.9 m^3/s and the third one for a discharge of 1.4 m^3/s. The conceptual model of the investigated system remains the same, the parameters were adapted to each tracer test. Fig. 8 shows the output BTCs (obtained at the system exit C) from tracer-test 1, 2 and 3 and the optimized fitted curves corresponding.

Parameters values estimation are summarized in Table 1. In each case, C_r and P_e numbers have values inferior to 1, which attests that the simulations are stable. On the transport parameters, a few first conclusions can be drawn.

Table 1
Modelling of the traced system in different flow conditions (tracer-tests 1, 2 and 3): dimensioning and transport parameters estimation.

Q (m^3/s)	Reach	Optimized parameters				Calculated from the parameters				Model stability	
		A (m^2)	A_s (m^2)	D_L (m^2/s)	α (s^{-1})	Vol (m^3)	Vol_s (m^3)	V_e (m/s)	a_L (m)	C_r	P_e
0.7	**1** Flooded area	34.2	22.0	0.102	3.9E−04	9180	5940	0.020	4.5	0.02	0.07
	2 River stretch	17.0	/	0.683	/	11,050	/	0.041	16.6	0.03	0.01
	3 Flooded area	43.3	7.5	0.174	1.6E−05	26,240	4545	0.016	10.8	0.01	0.02
0.9	**1** Flooded area	36.6	23.5	0.085	1.0E−04	9880	6345	0.024	3.5	0.02	0.07
	2 River stretch	20.0	/	0.51	/	13,000	/	0.045	11.3	0.03	0.03
	3 Flooded area	45.4	8.9	0.108	1.3E−04	27,270	5340	0.019	5.7	0.01	0.04
1.4	**1** Flooded area	37.0	26.0	0.13	7.2E−05	9990	7020	0.038	3.4	0.02	0.07
	2 River stretch	22.2	/	0.72	/	14,440	/	0.063	11.4	0.02	0.01
	3 Flooded area	45.0	10.3	0.12	6.8E−05	27,270	6242	0.030	4	0.01	0.01

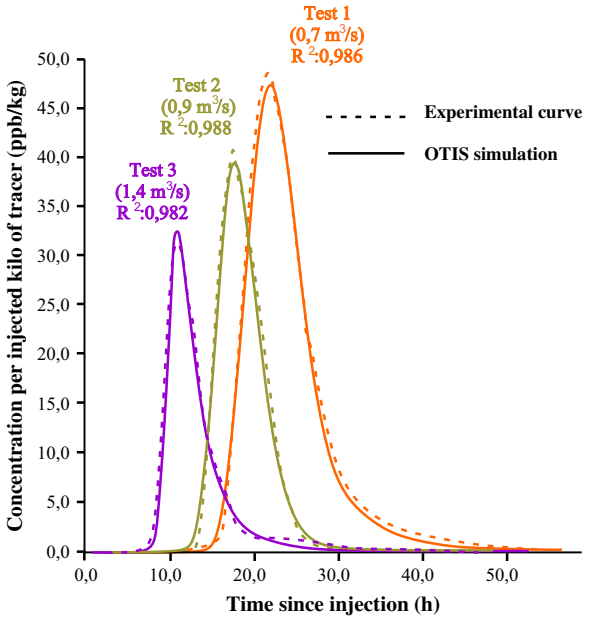

Fig. 8. Comparison of the experimental output BTCs and the OTIS simulated curves for each tracer-test. Note that the concentration is expressed in ppb per injected kilo of tracer. The modelled system is the GB–C system that is discretized in three reaches.

5.2.1. Main flow section (A)

The modelled dimensions seem reliable, all the more since the active river stretch section between locations B and C (reach 2) was evaluated on the field showing that in situ measures are similar to the OTIS values. Furthermore, as it could be expected, A values are much bigger for the flooded areas than for the active river. In consequence, effective velocity (V_e) is at least two times higher in the river section. Moreover, A in flooded areas does not vary in a significant way whatever the flow conditions while in the river stretches it increases with flow.

5.2.2. Storage zone section (A_s)

OTIS confirms that the modelling of solute transport in flooded areas needs to suppose the existence of a storage zone (immobile water) in which solute can be caught. On the contrary, immobile water in the river stretch is considered as non-exist in the model. A_s, and so the volume of the storage zone, is smaller than the main flow volume in both reach 1 and 3. However, considering the total volume of water affected by the tracer cloud; i.e. $Vol + Vol_s$, the immobile water constitutes 35–41% of this total volume in reach 1 but only 12–15% in reach 3. So the volume of immobile water is not influenced by the volume of the flow section.

Finally, unlike the main flow section, A_s is apparently dependent of the flow conditions as shown by the As value difference between tracer-test 1 and 3. Therefore, flooded areas have to be thought as fracturated rock volume in which the main flow section is constrained whatever the flow but where the volume of immobile water can increase with a growing discharge. Fig. 9 proposes a conceptualization of flooded areas in Han-sur-Lesse.

5.2.3. Exchange coefficient (α)

In OTIS, α is described as the fraction of the main channel volume that is exchanged with the storage zone, per unit time. So α constrains the mass of solute that will be exchange between mobile and immobile zone. The α values modelled by OTIS in the Han-sur-Lesse case vary between 1.6×10^{-5} and $3.9 \times 10^{-4}\ s^{-1}$. Comparing to α values found by Field and Pinsky (2000), i.e. 1.0×10^{-5} to 5.0×10^{-5}, or Geyer et al. (2007); i.e. $2.5 \times 10^{-6}\ s^{-1}$, α in the Han-sur-Lesse system is slightly higher. There is no clear evolution tendency in the α values in regard to the discharge changes, and α stays rather stable in the different reach. It seems therefore that the exchange coefficient is not very dependent to the storage volume or flow conditions, at least in the range of discharge considered in this study.

5.2.4. Dispersion coefficient (D_L)

Simulated D_L values vary between 0.085 and 0.72 m^2/s. There is no clear trend in the D_L values evolution between the tests. Theoretically, the dispersion coefficient should increase when the flow increases. Indeed, several authors (Hauns et al., 2001; Massei et al., 2006; Morales et al., 2010) have shown that the relation $D_L = a_L \cdot V_e$ is verified in karst conduits. In our case, this relation is not so evident but one should keep in mind that the range of discharge in which the tests were performed is rather small. Actually, in the low flow conditions that characterized our field experiment, D_L seems more inherent to the type of environment than to the general flow conditions. Indeed, the river stretch has, in each case, a more dispersive behavior than the flooded areas. This fact can be

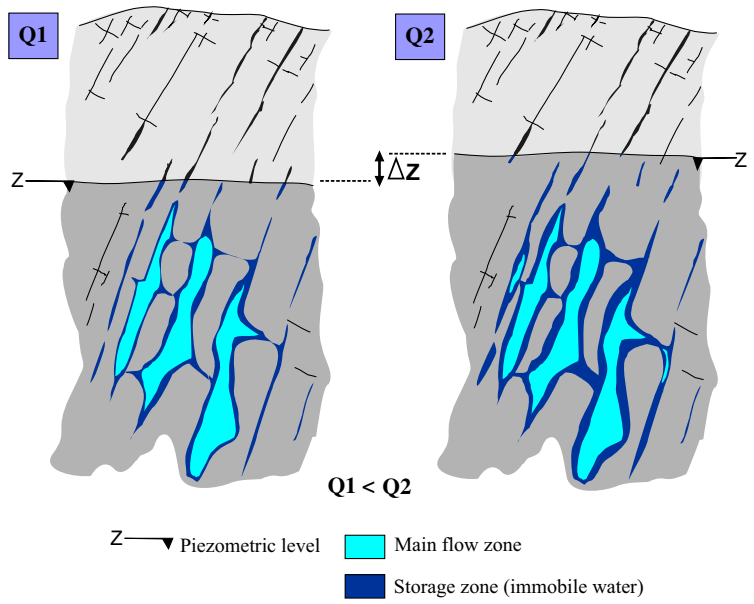

Fig. 9. Flooded area conceptualization deduced from the modelling results. Main flow zone in flooded area is confined while the storage volume grows with the discharge (modified from Bonniver, 2011). The sketch is without scale.

easily understood, considering that velocity is much higher in the river given that the section is smaller. Turbulence effects along the walls are then presumably more important in the river stretches than in the flooded areas, giving way to higher dispersion. Furthermore, the absence of immobile water in the river stretches, which was stated from the field observation and confirmed by the modelling, should also explain the higher dispersion. Indeed, immobile water being logically concentrated along the rock walls, the storage section could be seen as a buffer zone that mitigates turbidity and thus dispersion. This immobile water being absent of the river stretches, there is no buffering action that could decrease turbidity.

5.3. Transport characterization in flooded areas

5.3.1. Sensibility tests

As the BTC's characterizing solute transport through the system GB–C are quite symmetric, the effect of immobile water present in flooded area is not easy to distinguish on the curves. Indeed, if the flaring and the asymmetry of the BTCs increase along the path, the tailing effect generally linked to retardation is not very clear. This is probably due to the equilibrium between residence time in storage zone and restitution time. In fact, when transport in the main flow zone is too quick or that the travel distance is too short, storage is not really effective because the contact time between mobile and immobile water is too short for it to develop (Brouyère, 2001; Zhang et al., 1998; Wang, 1987). Hauns et al. (2001) showed that retardation and dispersion are much more important in systems where dispersive structures (pool, rapids) exist, and that those processes are the expression of a transient storage. Nevertheless, the effect on BTCs is rather complex because of the "scale effect" which implies that retardation is dominant at a local scale but that it will decrease for the benefit of dispersion with growing length scale (Jeannin and Maréchal, 1997). This is explained by the fact that storage time becomes smaller than restitution time when distance increases. To resume, breakthrough time has to be long enough to allow the development of transient storage but not too long at the risk of becoming longer than the residence time in storage zone.

In the attempt to understand the hydrodynamic of the transport parameters in flooded areas particularly, sensibility tests were performed on reach 1 and 3. As they both showed similar responses to the sensibility tests, results presented here (Fig. 10) are those of the tests leaded on reach 1 only. They consist in varying one parameter at a time, the three others staying constant. Fig. 10 shows for each parameter the initial OTIS fitted curve and the resulting curve obtained from the parameter variation. The deviation of the new curve from the initial model can be assessed visually and mathematically thanks to the determination coefficient. Given the really good result of our initial modelling (R^2 superior to 0.991), it will be considered that a R^2 inferior to 0.980 corresponds to a significant deviation. Fig. 10 indicates a strong control of the main flow section on the result (Fig. 10A). Indeed a change of +10% or −10% of the A initial value is enough to lower R^2 to 0.961 and 0.957 respectively. In varying the A value, the first arrival and the peak concentration are greatly impacted. It can therefore be considered that the initial A value is accurately estimated within an error margin of less than 10% of its value. The storage zone section estimation seems also to have a major influence on the BTC shape but it is a bit less sensible than A as a change of at least 20% of its initial value is needed to lower R^2 to less than 0.980. (Fig. 10C). The BTC changes are seen mainly in the first arrival and the peak concentration as well. Variation of D_L (Fig. 10B) and α (Fig. 10D) values has an impact on the peak concentration mainly. They are however much less sensible as in the D_L case, a change of more than ±50% of the value is necessary to see a significant deviation (R^2 under 0.980) from the fitted curve.

In addition to assessing the sensibility of the different parameters, those tests show also interesting things in regard to the BTC shape, especially concerning the tailing effect. Eq. (3) governing the evolution of concentration in the storage zone should be kept in mind during the following analysis. In this equation, we will suppose an initial situation where solute concentration in the main flow zone is superior to the concentration in the storage zone, therefore the gradient considered implies an accumulation of solute in the storage zone. Solute restitution from the storage zone to the main flow zone happens when $C_s > C$. Looking at Fig. 10A, strong asymmetry and important retardation appear on the curve when A comes down to half of its initial value, which means in case of reach 1 that A is set to 17.1 m^2. Reaching this value, A becomes even smaller than A_s (22 m^2). Eq. (3) involves that a diminution of A

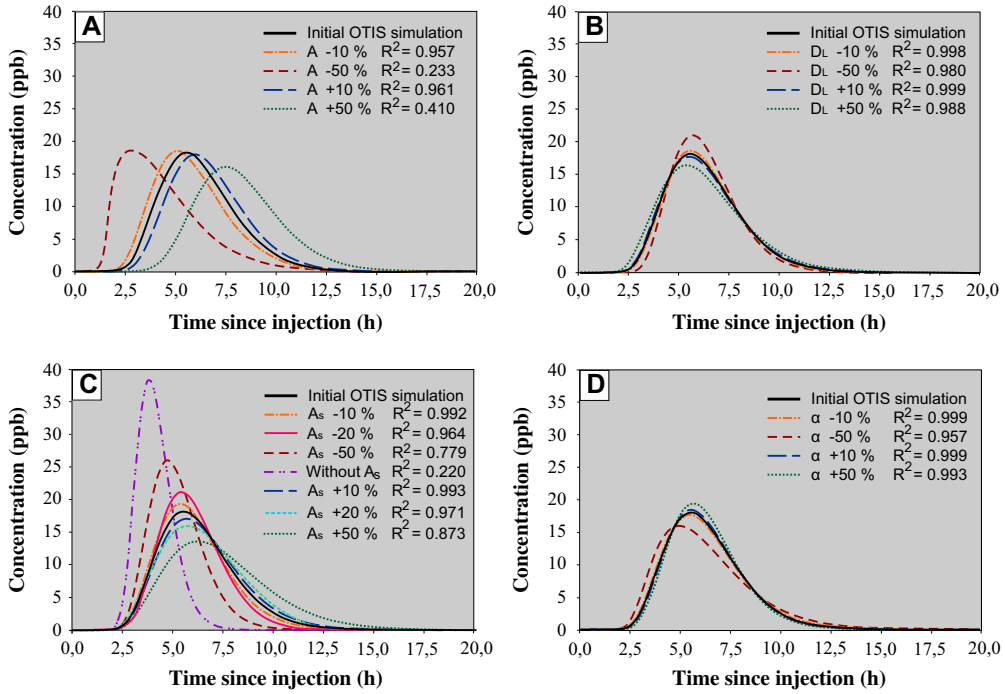

Fig. 10. Parameters sensibility tests for reach 1 modelled in tracer-test 1. Each graph corresponds to one different parameter: (A) flow zone section; (B) dispersion coefficient; (C) storage zone section; (D) transient storage coefficient.

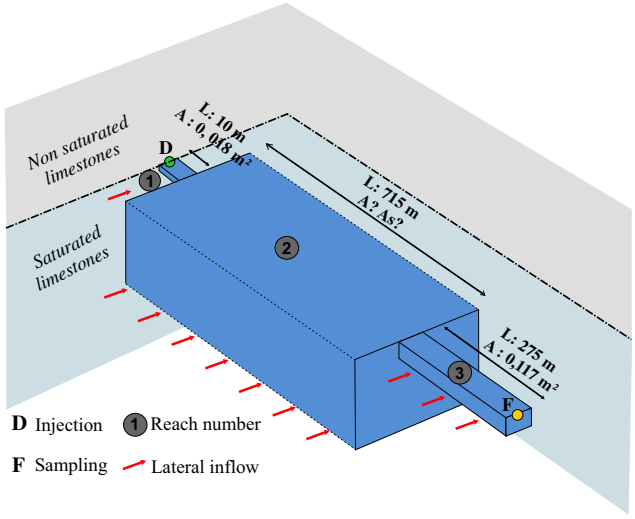

Fig. 11. Conceptual model of the D–F system. Reaches 1 and 3 are river stretches (RS) whose section are known while reach 2 is a big flooded area (FA) of unknown geometry.

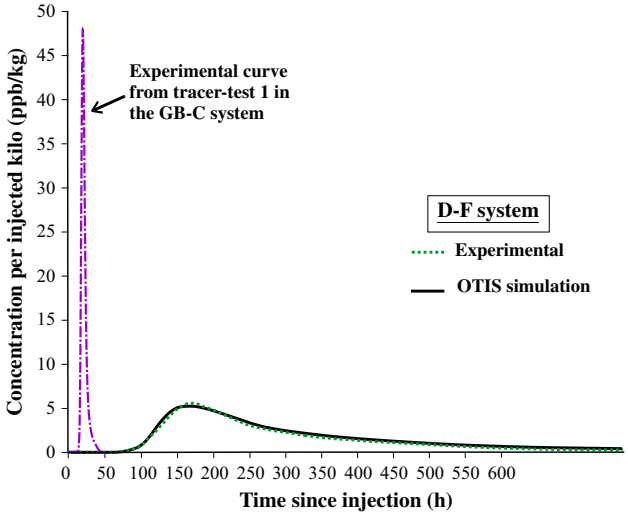

Fig. 12. Experimental and simulated BTC from the tracer-test performed on the D–F network. In comparison, the exit BTC from tracer-test 1 is also present on the graph.

slows down the accumulation rate in the storage zone, delaying the moment where $C_s > C$ and then prolonging the solute residence time in the storage zone. In these conditions, transient storage in immobile water is translated in tailing effect due to a breakthrough time that has become shorter than the residence time in storage zone, and, on the other hand, first arrival comes earlier. On the contrary, on the "A + 50%" curve, retardation tends to disappear probably in the benefit of dispersion (flattering and widening of the curve).

When looking at the sensibility test on D_L, it seems clear that changing the dispersion coefficient has no real impact on the tail of the curve but only on the widening of this one and on the peak concentration. More or less dispersion contributes to having a more or less concentrated cloud of tracer in the main flow zone but would not impact the transient storage.

The behavior of the BTC in relation to A_s and α has to be examined. It is clear through Fig. 10 that the presence of a storage zone is necessary to fit the simulated curve to the experimental one. Adding transient storage increases retardation as tailing is clearly growing with A_s. Retardation becomes evidently a major process of the transport on the "A_s + 50%" curve. This evolution is in accord with Eq. (3) which states that evolution of concentration slows when A_s increases and therefore breakthrough time becomes shorter than the residence time in storage zone. One could propose that a bigger volume of immobile water dilutes solute concentration and delays the restitution of the solute to the main flow. However, when looking at the last graphic that concerned α sensibility,

Table 2
Parameters value estimation from the OTIS simulation on the D–F system.

Reach	Optimized parameters				Calculated from the parameters				Model stability	
	A (m^2)	A_s (m^2)	D_L (m^2/s)	α (s^{-1})	Vol (m^3)	Vol_s (m^3)	V_e (m/s)	a_L (m)	C_r	P_e
1 River stretch	0.018	/	5.43	/	0.18	/	1.11	4.89	0.04	0.10
2 Flooded area	23.0	40.0	0.05	1.8E−06	16,445	28,600	0.0013	38.5	0.001	0.01
3 River stretch	0.117	/	4.36	/	32.2	/	0.29	15	0.01	0.03

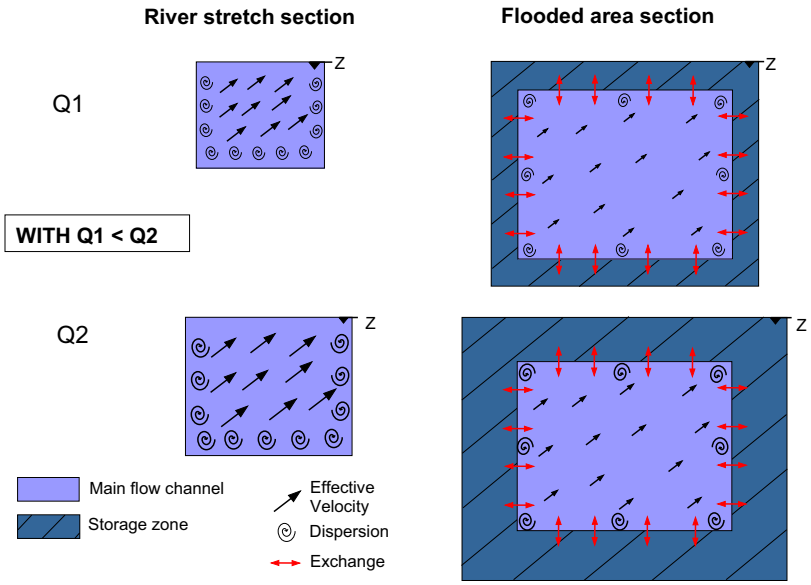

Fig. 13. Comparison of the transport parameters evolution in river stretch and flooded area when discharge increases. The size of the symbols reveals the intensity of the different processes. The scheme is without scale.

it can be seen that rising α with A_s stable has no impact on the tailing but has a small effect on the peak concentration of the BTC which is slightly higher. That could be explained in thinking that the storage zone becomes saturated in solute more quickly when α increases which favor the setting of a gradient releasing solute from the storage zone to the main flow. Solute trapping in the storage area is not long enough to cause real retardation. The fact that the global shape of the BTC is not really affected by a growing α is probably linked to a maximum storage capacity in the defined volume of immobile water; i.e. the mass released in the main flow zone will be limited to an upper value that could not change much the peak concentration in the main channel. In contrast, a significant decrease (−50%) of α modifies the restitution by growing the BTC asymmetry and the tailing effect. Indeed, storage zone will take more time to release the caught solute in the flow channel allowing retardation to affect the solute transport.

5.3.2. Application to an another case study

In order to compare the simulation results and to confirm the role of flooded areas, an additional tracer-test was performed on a small tributary network in Han-sur-Lesse where the tracer will flow mainly through a flooded area. The system traced, that we will call the D–F system (Fig. 11), starts with an accessible underground river stretch whose section could be measured and evaluated at 0.018 m^2. Then, this streamlet flows into a huge flooded zone whose features are unknown. Tracer sampling was performed in a conduit (measured section of 0.117 m^2) 275 meters downstream the flooded area. A discharge difference was observed between the injection point (0.02 m^3/s) and the sampling point (0.034 m^3/s). The additional 0.014 m^3/s have been attributed to natural aquifer drainage by the karstic system (Bonniver, 2011). The experimental BTC (Fig. 12), set at a restitution rate of 100%, shows a strong asymmetry and tailing. This suggests an important retardation that could be due to the flooded area crossing. An OTIS simulation was therefore performed to dimension the traced system, especially the flooded area. However, for technical reasons, there is only one sampling point at the exit of the system. Therefore, there was no intermediate curve available for a first calibration and the modelling was performed directly on the system as a whole. This is possible with OTIS as long as the system is not too complex. Furthermore, in this case, dimensions of the two river stretches sections were measured on the field. Heterogeneity of the D–F system allows representing it in a conceptual model made of three reaches (Fig. 11): a river stretch of 10 m length followed by a flooded area long of 715 m and finally a river stretch long of 275 m. A steady flow of 0.02 m^3/s is set at the upstream boundary while a lateral inflow of 0.000014 m^3/s m is spread on the total system length (1000 m). Modelling results are shown in Table 2 and Fig. 12.

As in the GB–C system, a storage zone needs to be simulated in OTIS to fit the modelled BTC to the experimental one. In the D–F system case, OTIS evaluates a main flow section of 23 m^2 for a storage zone section of 40 m^2. The flooded area has then a storage zone whose volume is 40% bigger than the main flow zone volume. The coefficient that regulates exchanges between the main conduit and the storage area has a fitted value of 1.8×10^{-6} s^{-1}. The combina-

tion of a huge storage zone and a small exchange coefficient explain the important retardation observed on the BTC because it extends the residence time in the storage zone as shown by the sensibility tests above. In order to compare the two systems, the tracer-test 1 BTC from the GB–C system was added in Fig. 12. The flooded area modelled in the D–F system is much less transmissive than those existing in the GB–C system and show a significant tailing. Concerning the dispersion coefficient, this simulation confirms that the conduit river type is clearly a more dispersive environment than the flooded area. One should notice that the value scale of D_L in those river stretches is much higher than in the GB–C system. That is linked to a quicker effective velocity in the D–F system. This simulation is consistent with the field observations and leads to the same conclusions that could be made on the parameters estimation in the GB–C system. This case study shows also that in a same global system (the Han-sur-Lesse system), flooded areas can act very differently on the solute transport and that the appearance of an important tailing effect is clearly linked to the system geometry.

Finally, in regard with the informations brought by this additional case study, and when summing up informations provided by the GB–C and the D–F simulations, a global scheme comparing flooded areas with underground river conduits can be proposed (Fig. 13):

- River stretches are highly transmissive environments where advection and dispersion are the main processes. They are mainly dependent of the flow conditions.
- Flooded areas consist in low velocity transport zone where dispersion moderates for the benefit of solute exchange with immobile water. Immobile water areas are located along the walls and act as buffer zones that mitigates turbidity and so, dispersion. Transient storage will result in retardation if the residence time in the storage zone is long enough. This parameter is strongly dependent of the flooded area geometry.
- The residence time in the storage zone is not necessarily longer when the flow increases but the storage capacity will grow with the discharge, while the main flow zone volume is rather constrained and the exchange rate stays steady.

6. Conclusion

The karstic system of Han-sur-Lesse is, as many other, very heterogeneous in its geometry. Indeed it combined transport in underground river stretches and in flooded areas. While the river stretches are usually accessible by speleologists, flooded areas are rather unknown given a limited physical access. This paper aim to define the geometry of those flooded zones and to characterize their effect on solute transport in comparison with the classical river stretches. In this purpose, multi-sampling sites tracer-tests were performed and the resulting BTCs were modelled via the OTIS program. The discrete system build with OTIS show a clear parametrization difference between the river stretches and the flooded zones. Indeed, flooded zones act as low transmissive environment where transport is dominated by the interaction with immobile water zones. The geometry of those zones, especially the ratio between the main flow section and the storage zone section is a major parameter that influences solute transport. Furthermore, the simulations and the sensibility tests demonstrate that the crossing of a flooded zone will give way to an important tailing only if the geometry and the exchange coefficient (α) allow the retardation to be longer than the restitution time. Actually, the direct effect of the storage on the tracer restitution is not systematic and seems clearly dependent on additional factors linked to the whole system functioning and geometry (presence of flooded areas and their geometry, flow conditions, system length,...). Finally, it can be said that conceptual models proposed by OTIS are, firstly, accurate and realistic and, secondly, strongly constrained by the BTCs which reflect the reality. Sensibility tests show that the OTIS model is stable because the fitting of the simulated curve to the real ones depends on an evaluation of parameters that is made in a narrow window of values. Equations that governed OTIS maintain the stability of the model and their resolution is highly dependent of the features of the investigated network. OTIS simulation gives informations on the system geometry which help to understand hydrodynamic processes that control solute transport in a specific network.

Acknowledgements

The authors would like to thank the limited company "Les Grottes de Han" and its members for the free access to the site and their interest in our work. A special thanks to Professor Yves Quinif who shared his knowledge of the Han-sur-Lesse karst with us. The writers are grateful to the University of Namur for supporting this research.

References

Blockmans, S., Dumoulin, V., 2016. Houyet-Han-sur-Lesse 59/1-2. Carte Géologique de Wallonie. Service public de Wallonie, DGO3 (Direction Générale Opérationnelle Agriculture, Ressources Naturelles et Environnement) (in press).

Bonniver, I., 2011. Etude hydrogéologique et dimensionnement par modélisation du « système-traçage » du réseau karstique de Han-sur-Lesse (Massif de Boine – Belgique). PhD Thesis, Département de Géologie, Facultés Universitaires Notre-Dame de la Paix (FUNDP), Université de Namur, Belgique, 349 p.

Brouyère, S., 2001. Etude et modélisation du transport et du piégeage des solutés en milieu souterrain variablement saturé: Evaluation des paramètres hydrodispersifs par la réalisation et l'interprétation d'essais de traçage in situ. PhD Thesis, Laboratoires de Géologie de l'Ingénieur, d'Hydrogéologie et de Prospection Géophysique, Faculté des Sciences Appliquées, Université de Liège (Ulg), Belgique, 572 p.

De Marsily, G., 1986. Quantitative Hydrogeology. Groundwater Hydrology for Engineers. Academic Press, New York, 440 p.

Donaldson, J.R., Tryon, P.V., 1990. User's Guide to STARPAC—The Standards, Time Series, and Regression Package: National Institute of Standards and Technology Internal Report NBSIR 86-3448.

Field, M.S., Pinsky, P.F., 2000. A two-region non equilibrium model for solute transport in solution conduits in karstic aquifers. J. Contam. Hydrol. 44 (3/4), 329–351.

Geyer, T., Birk, S., Licha, T., Liedl, R., Sauter, M., 2007. Multitracer test approach to characterize reactive transport in karst aquifers. Ground Water 45 (1), 36–45.

Gray, W.G., Pinder, G.F., 1976. An analysis of the numerical solution of the transport equation. Water Resour. Res. 12 (3), 547–555.

Hauns, M., Jeannin, P.-Y., 1998. Tracer transport in underground rivers in karst: tailing effects and channel geometry. Bull. d'Hydrogéol. 16, 123–142.

Hauns, M., Jeannin, P.-Y., Atteia, O., 2001. Dispersion, retardation and scale effect in tracer breakthrough curves in karst conduits. J. Hydrol. 241 (3–4), 177–193.

Havron, C., Vandycke, S., Quinif, Y., 2007. Interactivité entre tectonique méso-cénozoïque et dynamique karstique au sein des calcaires dévoniens de la région de Han-sur-Lesse (Ardennes, Belgique). Geol. Belgica 10 (1–2), 93–108.

Hubbard, E.F., Kilpatrick, F.A., Martens, L.A., Wilson Jr., J.F., 1982. Measurements of Time of Travel and Dispersion in Streams by Dye Tracing. Techniques of Water-Resources Investigations, Book 3, Applications of Hydraulics, chapter A9, US Geological Survey, Washington, DC.

Jeannin, P.Y., Maréchal, J.C., 1997. Dispersion and tailing of tracer plumes in a karstic system (Milandre, JU, Switzerland). In: Proceedings of the 12th International Congress of Speleology, vol. 2, La Chaux-de-Fonds, Switzerland, pp. 149–152.

Kinzelbach, W., 1986. Groundwater Modeling: An Introduction with Sample Programs in BASIC. Elsevier, Amsterdam, 333 p.

Maloszewski, P., Zuber, A., 1989. Mathematical Models for Interpreting Tracer Experiments in Fissured Aquifers. The Application of Isotope Techniques in the Study of the Hydrogeology of Fractured and Fissured Rocks, IAEA, pp. 287–301.

Maloszewski, P., Harum, T., Benischke, R., 1992. Mathematical modelling of tracer experiments in the karst of Lurbach system. Steirische Beiträge Hydrogeol. 43, 116–136.

Martin, J.L., McCutcheon, S.C., 1998. Hydrodynamics and Transport for Water Quality Modeling. Lewis, London, 794 pp.

Massei, N., Wang, H.Q., Field, M.S., Dupont, J.P., Bakalowicz, M., Rodet, J., 2006. Interpreting tracer breakthrough tailing in a conduit-dominated karst aquifer. Hydrogeol. J. 14 (6), 849–858.

Morales, T., Uriarte, J.A., Olazar, M., Antigüedad, I., Angulo, B., 2010. Solute transport modelling in karst conduits with slow zones during different hydrologic conditions. J. Hydrol. 390 (2010), 182–189.

Quinif, Y., 1988. Structure hydrogéologique du Massif de Boine. Lapiaz, Han special number, 11–14.
Rossier, Y., Kiraly, L., 1992. Effet de la dilution sur la détermination des dispersivités par interprétation des essais de traçage dans les aquifères karstiques. Bull. Centre Hydrogéol. Univ. Neuchâtel 11, 1–15.
Runkel, R.L., 1998. One-dimensional Transport with Inflow and Storage (OTIS): A Solute Transport Model for Streams and Rivers. USGS, Water-Resources Investigations Report, 98-4018, 73 p.
Runkel, R.L., Broshears, R.L., 1991. One-dimensional Transport with Inflow and Storage (OTIS): A Solute Transport Model for Small Streams. Boulder, Colo., University of Colorado, CADSWES Technical Report 91-01, 85 p.
Schnegg, P.A., Doerfliger, N., 1997. An inexpensive flow-through field fluorometer. In: Proceedings of the 6th Conference on Limestone Hydrology and Fissured Media, vol. 2, La Chaux-de-Fonds, August 1997. Centre of Hydrogeology, University of Neuchatel, pp. 47–50.
Wang, H., 1987. Modélisation des transferts de masse en milieu saturé à double porosité; application aux écoulements convergents en craie fissurée et multicouche. PhD Thesis, University of Paris XI, Paris.
Werner, A., Hoetzl, H., Käss, W., Maloszewski, P., 1997. Interpretation of tracer experiments in the Danube-Aach-System (Western Swabian Alb, Germany) with analytical models. In: Günay, Johnson (Ed.), Karst Waters Environmental Impacts. Balkema, Rotterdam, pp. 153–160.
Zhang, H., Schwartz, F.W., Wood, W.W., Garabedian, S.P., LeBlanc, D.R., 1998. Simulation of variable-density flow and transport of reactive and nonreactive solutes during a tracer test at Cape Cod, Massachusetts. Water Resour. Res. 34 (1), 67–82.